Thermal characterisation of a boiling-meter using experiment and numerical simulation in a boiling cell

Abdelkabir ZAITE[1], Himanshi KHARKWAL[2], Magali BARTHES[2], François LANZETTA[3], Hervé COMBEAU[4], Lounès TADRIST[1]

[1]Université d'Aix-Marseille, CNRS, IUSTI, Marseille, France
[2]Université de Franche-Comté, CNRS, Institut FEMTO-ST, F-25000 Besançon,
[3]Université de Franche-Comté, CNRS, Institut FEMTO-ST, F-90000 Belfort, France
[4]Université de Lorraine, CNRS, Institut Jean Lamour, Nancy Cedex, France

abdelkabir.ZAITE@univ-amu.fr[1], *himanshi.kharkwal@univ-fcomte.fr[2], magali.barthes@univ-fcomte.fr[2], francois.lanzetta@univ-fcomte.fr[3], herve.combeau@univ-lorraine.fr[4], lounes.tadrist@univ-amu.fr[1]*

Abstract: In this paper, a method for calibrating a boiling-meter is carried out. It uses a combined experimental and numerical simulation approach to ensure consistency of results. For this, experiments were carried out in a boiling cell containing a Fluorinert (FC-72) liquid topped with a gas canopy. The liquid is heated using a heat source installed in a boiling cell, enabling heat transfer to be measured at the surface of the cell walls. Experiments were carried out under well-controlled operating conditions. The experimental results obtained were compared with literature correlations. Good agreement was observed under certain conditions in steady state conditions, but often with limited precision. Numerical simulations of the experiment were carried out using Star CCM+ software. They take into account convection flows in three-dimensional geometry. The results of the numerical and experimental simulations are found to be in good agreement over the whole of the warm-up period until a steady state is reached. The robustness of these results led to an analysis of convection flows in the experimental cell. Preliminary results have revealed flow structures that explain the differences in heat transfer to the walls depending on the orientation of the boiling-meter relative to gravity.

Keywords: Heat transfer, Boiling-meter calibration, experiment, 3D Numerical Simulation, Natural convection, flow pattern

1 Introduction

Boiling is an efficient way of thermal management in various applications like power electronics, nuclear reactors and space missions [1]. Thus, a lot of studies are conducted focusing on different boiling parameters like heat transfer rate, heat transfer coefficient, and critical heat flux. However, to understand the physics of boiling, one must be aware of how accurate the temperature and heat flux monitoring techniques are. Moreover, it is also required to get as much information as possible about the structure of the flow and the temperature field in the vicinity of the heated surface. The different techniques adopted by the researchers for calculating heat flux are: 1. Placing temperature sensors in a material (with known conductivity) at a known distance and using Fourier's law [2]; 2. Inferring heat flux from the current and voltage values provided by the power supply given to the heater, while assuming no losses occur during the energy conversion via Joule heating [3, 4]; 3. Using infrared cameras [5]; and 4. Using heat flux sensors [6]. The first two methods are the most often employed by researchers; nevertheless, they are not suitable for studying the boiling phenomenon in non-steady state conditions, particularly for analysing bubble behaviour. Furthermore, boiling phenomena can be studied at very low heat fluxes by utilizing infrared cameras; however, since this approach is new, it is not well-advanced for boiling applications. Thus, to study bubble parameters during incipience, growth, and departure phases, researchers are recently developing novel methods. One such method for this purpose is the use of heat flux sensors [7, 8]. Using high frequency heat flux sensors, parameters for each bubble could be analysed. In light of this, the current study represents a step toward the analysis of a "boiling-meter". The boiling-meter is a device that provides a boiling surface and permits surface orientation changes during the pool boiling phenomenon. It is equipped with sensors which give instantaneous measurements of the surface temperature and heat flux rate.

Our general purpose in the current work is to develop a boiling-meter to analyse the phenomenon of phase change, and nucleation at the onset of nucleate boiling in non-stationary conditions. For this aim, it is important to calibrate the boiling meter developed in steady and non-steady state conditions. As the study configuration is complex, it is important to have calibration tools adapted to the situation under study. In the present configuration,

the boiling-meter is placed at the heart of the liquid in the experimental reference cell. The heating caused by the heating element inside the boiling-meter will generate natural convection phenomena in the fluid, which will drive the heat transfer between the fluid and the wall. Calibration using correlations established in the literature is at first adopted approach. This approach is limited to the particular configuration under study. Therefore, a numerical simulation tool to predict the conjugate heat transfers in the boiling-meter (solid), and in the fluid where natural convection may take place is developed taking into account the geometry of the cell.

Huge work has been done previously by researchers to analyse heat transfer through natural convection, and especially to study the flow patterns using numerical simulation [9]. Natural convection is a well-known phenomenon, and several numerical codes can simulate it [10]. In the present study, experiments enabling natural convection heat transfer are carried out and are evaluated and analysed using numerical simulation. For this aim, a 3-dimensional CFD model is developed in the commercial code Star CCM+. Such a model helps in performing the calibration of experimentally examined boiling-meter, while analysing the heat transfer on the boiling-meter wall and the flow pattern induced in natural convection. In this paper, the experimental results as well as numerical ones are presented for the boiling-meter calibration. Preliminary results on the flow pattern and the temperature field are also discussed.

2 Experimental setup and protocol

The experimental device used here is designed to have well-controlled operating conditions. It consists of a cuboid cell (see Fig. 1) having dimensions of 15 cm x15 cm x 17 cm and a thickness of 2.5 cm. It is designed to work in a pressure range of 0.03 bar to 3 bar. The whole structure of the test cell is made of plexiglass, which allows the minimisation of heat losses and also gives the benefit of visualisation from all sides. Furthermore, to provide the boiling surface and study the effect of inclination, the test cell is equipped with a rotating boiling meter. This boiling meter is composed of two identical heat flux sensors, thermocouples, and a heating resistance. The heat flux sensors are circular discs with a diameter of 2 cm and a thickness of 0.4 mm. The sensitivity of the heat flux sensor is 2.94 µV/W/m^2. The wall temperature is measured thanks to K-type thin-film thermocouples (30 µm of thickness) deposited at the center of the top and bottom faces of the boiling-meter. Moreover, to minimise the lateral heat losses, an insulation resin is molded in the periphery of the boiling meter. The test fluid studied is Fluorinert (FC-72). Further, K-type wire thermocouples are equipped in the test cell to measure the temperature of the bulk liquid. A data acquisition system "Multichannel Recorder DAS240BAT, SEFRAM" is used to measure and record the temperatures, powers, and heat flux densities. The schematic of the experimental setup is shown in Fig. 1.

The experimental protocol adopted is to achieve heat transfer at the boiling meter surface. Thus, electrical power between 0.3 W and 1.4 W is provided to the heating resistance. The experimental procedure adopted for carrying this study is- firstly the experimental setup is filled two third with the FC-72 topped with a gas canopy; and further boiling meter is set to the surface inclination of 0°. Following that, the boiling meter receives its initial electrical power of 0.3 W, which is then maintained until stationary conditions are reached. At that point, the heater's input power is increased to 1.4 W. The data acquisition system recorded the wall temperature and heat flux during the entire experiment, and it was then utilized to compare the results with the heat flux and wall temperature acquired from the numerical simulation.

3 Numerical simulation

The physical model of the of the enclosure and the boiling-meter are shown in Fig. 1 (a) and (b). The parameters of the modelled system are the same used in the experiment.

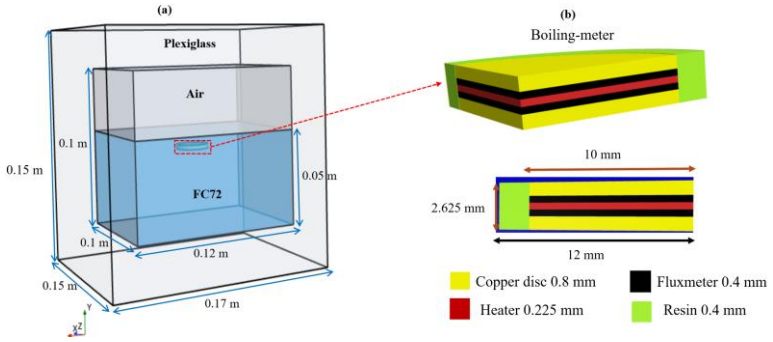

Figure 1: Schematic representation of the test cell and the boiling-meter used for numerical simulation. The thermophysical properties of the cell components are: copper disc (λ=398 W/(m K), c_p=386 J/(kg K), ρ=8900 kg/m^3), fluxmeter: (λ=0.4 W/(m °C), c_p=693 J/(kg °C), ρ=4920 kg/m^3), heater: (λ=0.225 W/(m °C), c_p=1012 J/(kg °C),

ρ=2251 kg/m^3), resin: (λ=0.25 W/(m °C), c_p=1000 J/(kg °C), ρ=1000 kg/m^3), plexiglass: λ=0.19 W/(m °C), c_p=1470 J/(kg °C), ρ=1190 kg/m^3), FC-72: λ=0.051 W/(m °C), c_p=1102 J/(kg °C), ρ=1620 kg/m^3)

3.1 Governing equations

To calibrate the boiling-meter using numerical simulation, the heat transfer phenomena in the boiling cell, which comprises the boiling-meter, the fluids present and the walls of the enclosure (Figure 1), are considered in the problem formulation. The presence of the heating element in the boiling-meter makes it possible to generate heat flux through the circular base and lateral surfaces, thereby heating the fluid and the enclosure. It is then possible to induce natural convection flows in the fluids.

To study the phenomenon of natural convection, the model to be solved is based on the Navier-Stokes equations of incompressible fluid dynamics assuming a constant density of the liquid except in the buoyancy term of the momentum equation (Boussinesq approximation) coupled with heat and mass balance equations. Then, the continuity equation Eq.1, momentum equation Eq.2, and energy equation Eq.3. are written in indicial tensor notation as :

$$\frac{\partial u_i}{\partial x_i} = 0 \qquad (1)$$

$$\rho_{ref}\left(\frac{\partial u_i}{\partial t} + u_j \frac{\partial u_i}{\partial x_j}\right) = \frac{\partial}{\partial x_j}\left(\mu \frac{\partial u_i}{\partial x_j}\right) - \frac{\partial p}{\partial x_i} + \rho_{ref} g_i \left(1 - \beta_T \left(T - T_{ref}\right)\right) \qquad (2)$$

$$\rho_{ref} c\left(\frac{\partial T}{\partial t} + u_i \frac{\partial T}{\partial x_i}\right) = \frac{\partial}{\partial x_i}\left(\lambda \frac{\partial T}{\partial x_i}\right) \qquad (3)$$

Where x_i (x, y, z) are the space coordinate, u_i (u_x, u_y, u_z) represents the velocity vector, T denotes the fluid temperature, ρ_{ref} is the fluid density at the reference temperature T_{ref} , β_T the thermal expansion coefficient, p the pressure, μ the dynamic viscosity of the fluid, c_p the specific heat capacity of the fluid, and λ is the thermal conductivity.

This formulation assumes that the natural convection regime is laminar. This assumption has been checked a posteriori for the two cases studied. Indeed, the Rayleigh number ($Ra = \frac{g\beta_T \Delta T l^3}{\nu\chi}$) calculated do not exceed 1.6 10^7 (see § 4).

In the boiling-meter and the cell walls, the energy equation takes the same form than Eq.3 without the convective term and adding a source term to account for the heat release by the electric resistance. It comes:

$$\rho c \frac{\partial T}{\partial t} = \frac{\partial}{\partial x_i}\left(\lambda \frac{\partial T}{\partial x_i}\right) + q \qquad (4)$$

The physical model used in this work has been discretized thanks to the three-dimensional computational fluid dynamics (CFD) software Star CCM+. Equations 1-3 and 4 are discretised using the finite volume method with a first-order scheme for the convective and diffusive terms and a fully implicit time integration scheme. The coupled system of equations is solved with a Newton-Raphson iterative procedure and the linear systems with a conjugate gradient method at each iteration.

3.2 Domains definitions and meshes

As indicated before, the test cell is composed of a Plexiglas enclosure containing a boiling meter, air, and FC-72 liquid. Thus, two fluid domains (FC-72 and air) and a solid domain (Plexiglas, boiling-meter components) are defined. The liquid FC-72 is considered an incompressible fluid, the contact between it and all solids is supposed perfect and non-permeable; no slip and no penetration are set as momentum boundary conditions for all solid walls ($u_i = 0$, $\partial u_i / \partial n = 0$). At the air-FC72 interface, perfect contact and continuity of the stress tensor are considered. The external walls of the cell are under convection conditions with ambient air of 22.5°C($-k \partial T / \partial n = h\left(T - T_a\right)$). The initial temperature of all cell components is ($T(x_i, t=0)=22.5$°C) at atmospheric pressure, according to experimental conditions. The initial velocity components of both fluids are zero ($u_i(x_i, t=0)=0$). In Eq. 4, perfect contact between solid components is assumed, with the variable q set to zero for all solid components except the heater, where it equals the imposed power in the experiments.

The computational domain was meshed using a trimmed cell Mesher defining a surface control allowing refinement at the thin boiling-meter components and the thermal boundary layer of FC-72. To study the mesh

sensitivity, the results for two meshes are presented. Mesh 1 is composed of 512027 cells while mesh 2 contains 1701154 cells. For both meshes, changing from one mesh to another is done by decreasing the refinement cell size. Fig. 2 (a) and (b) display images depicting the cross-sectional views of the boiling-meter and the surrounding FC-72 with mesh 1 and 2.

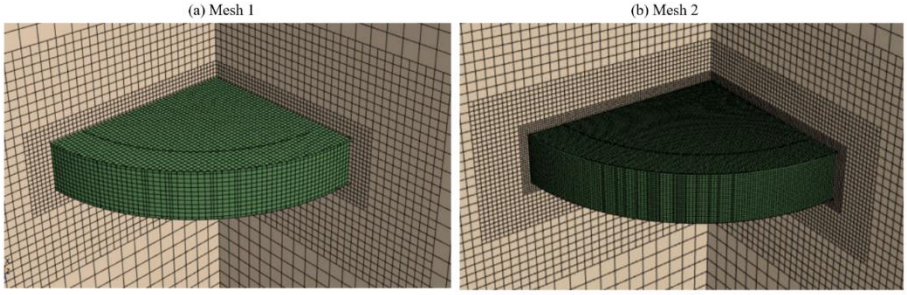

Figure 1: Image of meshes 1 (a) and 2 (b) of boiling-meter and surrounding FC-72.

3.2.1 Mesh analysis

In this part, numerical temperatures and heat flux from Mesh 1 and Mesh 2 are compared with experimental data to select the most suitable one for further numerical-experimental comparison. In the numerical model, the temperatures are calculated on the center circular base surfaces of the fluxmeters, and the heat flux are calculated on the contact surfaces between the fluxmeters and the copper modules. For both meshes, the simulations were performed with a time step of 0.1 s. Fig. 3 (a), and (b) present, respectively, a comparison between the experimental and numerical temperature and heat flux evolution versus time. Integral heat fluxes at the top and the bottom surfaces of the heater are plotted. One can see some differences between the results depending on the mesh. However, the results are not strongly dependent on the mesh and one can say that Mesh 1 is already a quite good discretisation in space. As the mesh is more refined in the region of the liquid close to the boiling-meter. The results of temperature and heat flux obtained using the Mesh 2 are in better agreement with the experimental results. This can be explained by the size of the Mesh 2 in FC72 in the vicinity of the boiling-meter. For this, we consider the Mesh 2 for analyzing the results.

The difference between the experimental and numerical results arises from the fact that the boiling-meter includes a handle that induces lateral heat losses. However, for simplicity in the numerical model, we have disregarded the boiling-meter handle, thereby excluding lateral losses.

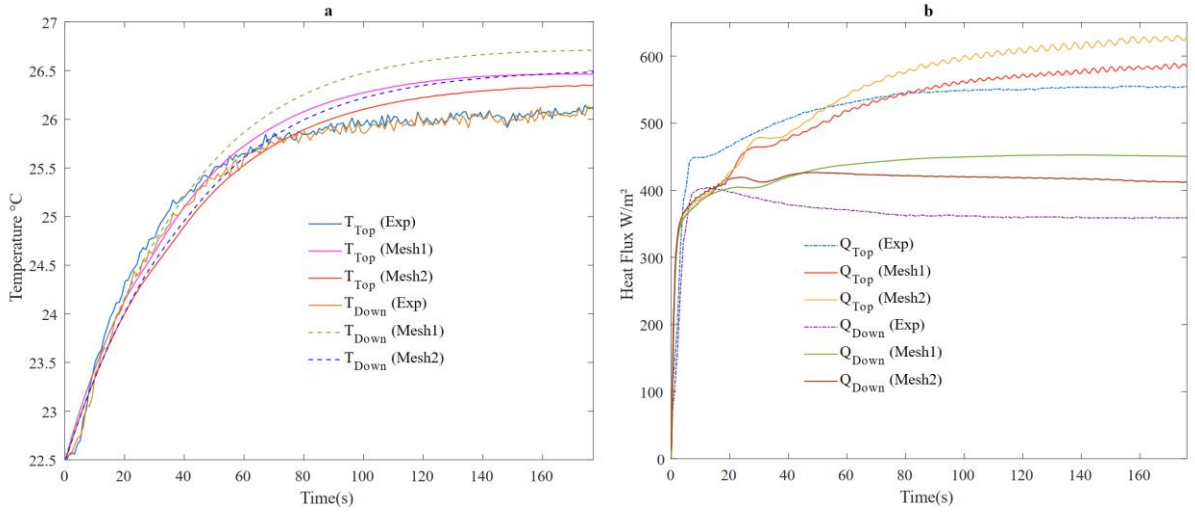

Figure 3: Temperatures (a) and heat fluxes (b) versus time. Experimental and numerical results obtained using the meshes 1 and 2.

4 Results and discussion

4.1 Heat flux and wall temperature

The wall temperature and heat flux for both sides of the boiling-meter are measured and evaluated using numerical simulation. Temperature and heat flux are measured at a depth of 800 µm from the surface of the boiling-meter

walls. Temperature is measured at the central point. The heat fluxes measured are those passing through the entire active surface of the 20 mm-diameter wall. Numerical results are compared for the same positions.

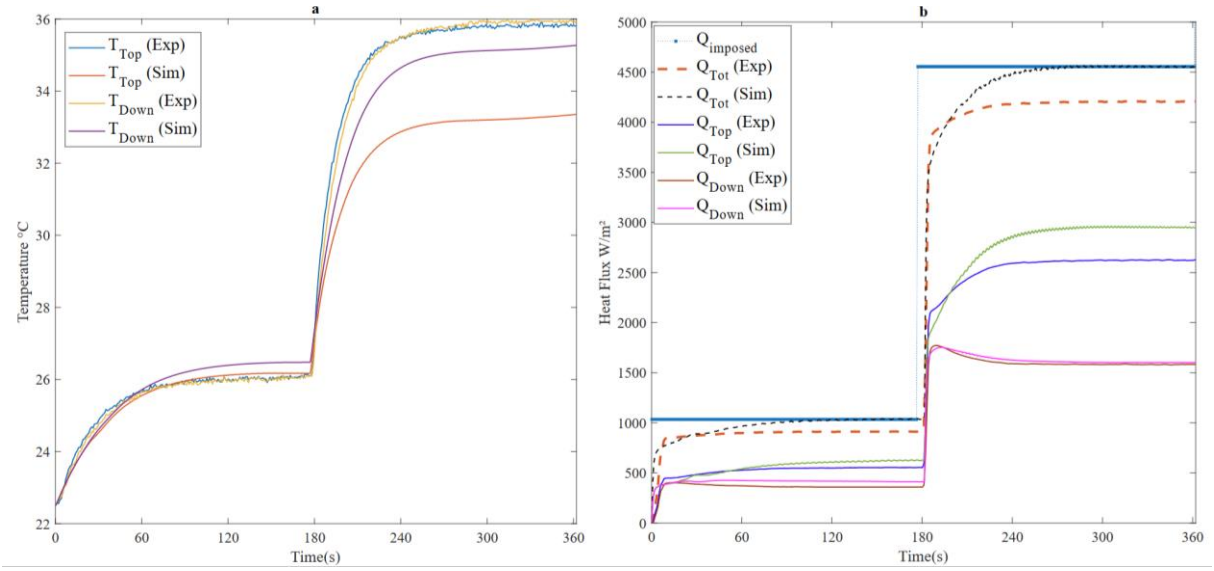

Figure 4: Temperature (a) and heat flux (b) variations versus time measured and predicted by numerical simulations. The coordinate of temperature is located at r=0 and z=-800µm from the wall surface. The heat flux is located at the same depth coordinate (z=-800µm). The subscript top corresponds to the wall where the fluid is above, while is the contrary for down.

It can be seen from the results shown in Fig. 4 that, there exists a good agreement between numerical and experimental results, for both wall temperature and heat flux for imposed total power 0.325 W. Response times are also well reproduced by the numerical simulation. At higher power 1.431 W there are a few discrepancies that can without no doubt be attributed to heat losses on the boiling-meter support not taken into account in the simulations and also simplifying assumptions (contact resistances between the various boiling-meter elements, neglect, etc.) which might play an important role at higher heat fluxes.

It can also be noted that, for low heat flux (0.325 W), the difference between upward and downward heat flux is small; and further as heat flux increases (1.431 W), the difference between upward and downward heat transfer increases. In the case of 0.325 W and 1.431 W, respectively, the upward heat transmission is over 20% and 40%. For wall temperature, this result is contrary, as when the heat transfer is higher wall temperature is lower. This can be explained by the convection phenomenon which occurs on the upside wall.

4.2 Fluid flow pattern

The good agreement between experiment results and numerical simulation is a good way to calibrate the boiling-meter and to ensure that the numerical simulation is well done and describes the physics.

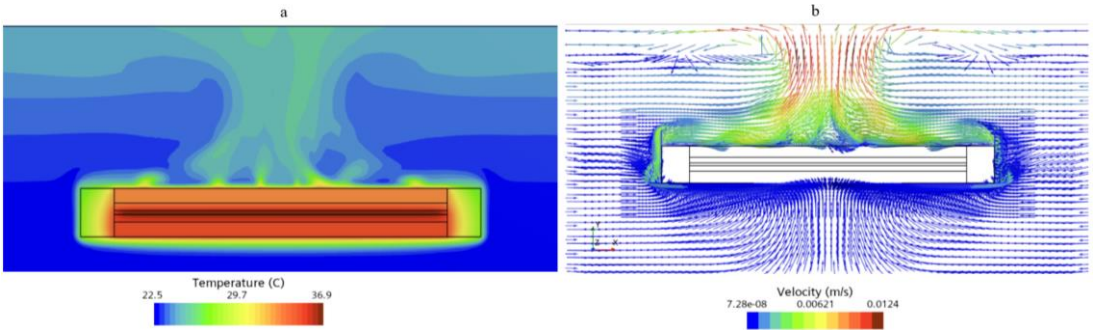

Figure 5: Instantaneous temperature (a) and velocity fields (b) in the boiling-meter and in the liquid in a vertical plane passing through the boiling-meter's mid-plane. This result corresponds to time t=362 s at the same time of Figure 4.

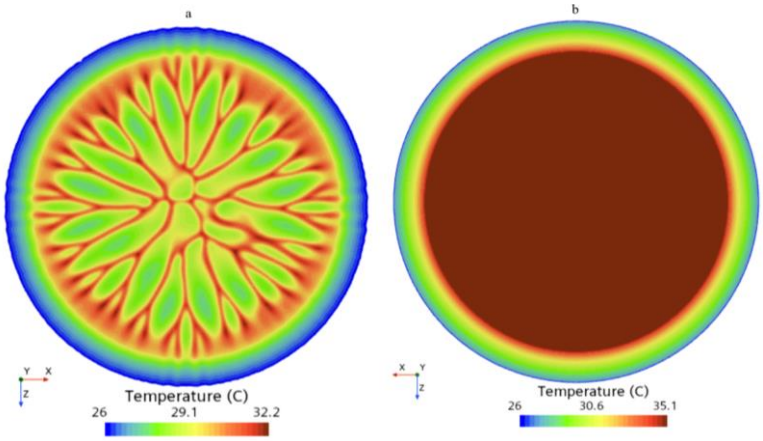

Figure 6: Instantaneous temperature fields in the liquid 100 µm from the top (a) and bottom (b) walls of the boiling-meter. This result corresponds to time t=362 s of the case presented in Fig. 4.

We observe from the temperature and velocity fields presented in Fig 5, that there is a non-symmetrical behaviour in the upward and downward faces. It is found that, for the upward face, fluid flows from the periphery of the boiling-meter to its center and then moves upward; while for the downward face, the fluid is quiescent. Moreover, the Fig.6 illustrates the complex nature of the induced fluid flow on the upper face. Plume emergence and disappearance are observed for a vertical plane associated with non-stationary convection.

5 Conclusion

We have carried out numerical simulations of heat transfer in a cell filled with a liquid topped by a gaseous overhead. The Joule-effect heat source in the boiling-meter can induce complex natural convection flows, depending on the intensity of the heat source. Numerical simulation using Star CCM+ software has enabled us to predict heat and momentum transfers in the measuring cell under conditions identical to those adopted in the experiment. The good agreement between the experimental and numerical results obtained for the cases studied confirms the consistency of the results obtained and validates the complementary nature of the approaches developed.

With these results, it is now possible to provide a detailed understanding of heat transfer between the fluid and the wall, and of natural convection flow structures in the cell.

Spatial-temporal variations in temperature and velocity have been demonstrated in the fluid. They differ according to the operating conditions. In the case of the horizontal orientation of the boiling-meter, structures develop in the form of unsteady "plumes" above the upper wall, with the appearance of temperature gradients in both horizontal and vertical directions. At the bottom wall, there is thermal stratification, and the liquid is in a "stable" regime. For a vertical orientation, the flow structure resembles three-dimensional convection rolls.

These results provide new insights and constitute a first step towards understanding heat transfer phenomena at the natural convection-transition-nucleation regime of vapor bubbles.

These numerical simulations will be extended to higher heat flux intensities, which can generate turbulent natural convection flows which will be investigated in a near future.

Nomenclature

Latin symbols

Symbol	Name	Unit
c	specific heat	J/(kg °C)
g	gravity	m/s^2
l	characteristic length	m
T	temperature	°C
u	velocity	m/s
p	pressure	Pa
Ra	Rayleigh number	
x ,y , z	space coordinates	m
t	time	s
Q	heat flux	W/m²
q	volumetric heat flux	W/m^3

Greek symbols

Symbol	Name	Unit
ρ	volumetric mass density	kg/m^3
λ	thermal conductivity	W/(m °C)
β_T	thermal expansion coefficient	1/°C
μ	dynamic viscosity	Pa s
χ	thermal diffusivity	m^2/s
ν	kinematic viscosity	m^2/s

Subscripts

Symbol	Name
a	air
ref	reference

Acknowledgements

The authors acknowledge Ass. Prof. Ahmed Kaiss and Engineer CNRS Lionel Meister for their helpful remarks for the numerical simulations. LT acknowledges the CNES (National Centre for Space Studies) and ANR – FRANCE (French National Research Agency) for its financial support of the TraThI project ANR-21-CE50-0009-01. This work has been supported by the EIPHI Graduate school (contract "ANR-17-EURE-0002"), by the Bourgogne-Franche-Comté Region and by the French RENATECH network and its FEMTO-ST technological facility.

References

[1] Falsetti C, Chetwynd-Chatwin J, Walsh EJ (2024) Pool boiling heat transfer of Novec 649 on sandblasted surfaces. International Journal of Thermofluids 22:100615. https://doi.org/10.1016/J.IJFT.2024.100615

[2] Yuan X, Du Y, Wang C (2023) Experimental study on pool boiling enhancement by unique designing of porous media with a wettability gradient. Appl Therm Eng 231:120893. https://doi.org/10.1016/J.APPLTHERMALENG.2023.120893

[3] Hutter C, Sefiane K, Karayiannis TG, et al (2012) Nucleation site interaction between artificial cavities during nucleate pool boiling on silicon with integrated micro-heater and temperature micro-sensors. Int J Heat Mass Transf 55:2769–2778. https://doi.org/10.1016/j.ijheatmasstransfer.2012.02.014

[4] Može M, Hadžić A, Zupančič M, Golobič I (2022) Boiling heat transfer enhancement on titanium through nucleation-promoting morphology and tailored wettability. Int J Heat Mass Transf 195:. https://doi.org/10.1016/j.ijheatmasstransfer.2022.123161

[5] Xia Y, Li R, Gao X, Li R (2023) Pool boiling on a biphilic surface where bubbles can move horizontally on the surface. Int J Heat Mass Transf 215:124540. https://doi.org/10.1016/J.IJHEATMASSTRANSFER.2023.124540

[6] Morisaki M, Minami S, Miyazaki K, Yabuki T (2021) Direct local heat flux measurement during water flow boiling in a rectangular minichannel using a MEMS heat flux sensor. Exp Therm Fluid Sci 121:. https://doi.org/10.1016/j.expthermflusci.2020.110285

[7] Zamoum M, Tadrist L, Combeau H, Kessal M (2014) Experimental Study of Boiling Heat Transfer on Multiple and Single Nucleation Sites Using a Boiling-Meter. Heat Transfer Engineering 35:508–516. https://doi.org/10.1080/01457632.2013.833052

[8] Tadrist L, Combeau H, Zamoum M, Kessal M (2020) Experimental study of heat transfer at the transition regime between the natural convection and nucleate boiling: Influence of the heated wall tilt angle on the onset of nucleate boiling (ONB) and natural convection (ONC). Int J Heat Mass Transf 151:119388. https://doi.org/10.1016/J.IJHEATMASSTRANSFER.2020.119388

[9] Fan Y, Zhao Y, Torres JF, et al (2021) Natural convection over vertical and horizontal heated flat surfaces: A review of recent progress focusing on underpinnings and implications for heat transfer and environmental applications. Physics of Fluids 33:. https://doi.org/10.1063/5.0065125

[10] Graževičius A, Bousbia-Salah A (2023) Comparative study of CFD and 3D thermal-hydraulic system codes in predicting natural convection and thermal stratification phenomena in an experimental facility. Nuclear Engineering and Technology 55:1555–1562. https://doi.org/10.1016/J.NET.2023.02.017